Binding of Transition-Metal Ions to Curved π Surfaces: Corannulene and Coronene†

Robert C. Dunbar

Chemistry Department, Case Western Reserve University, Cleveland, Ohio 44106

Received: January 31, 2002; In Final Form: May 13, 2002

Calculations and comparisons were made for a set of seven metal cations binding to corannulene and coronene, namely, the three alkalis Li^+, Na^+, and K^+ and the four transition-metal ions Ti^+, Cr^+, Ni^+, and Cu^+ (combined with literature results for Li^+/corannulene). In the case of corannulene, the most favorable binding site for Ti^+ and Ni^+ is η^6 over the six-membered ring on the convex face, whereas for Li^+, Na^+, K^+, and Cr^+, the five-membered η^5 ring site on the convex face is about equally good. Cu^+ slightly prefers binding at η^2 edge sites rather than ring-centered sites on corannulene, but edge locations for several other ions were not found to be favored, in contrast to results reported for C_{60}. For the alkalis, binding to the convex (outside) face is slightly favored relative to binding to the concave face, whereas for the transition metals, a much larger preference for outside binding is found, particularly for the η^5 sites. An approximate point-charge model calculation is used to separate the electrostatic-plus-polarization contributions to the binding to the η^5 sites from the electronic orbital contributions. Judging from this analysis, electronic orbital interactions favor outside binding of transition-metal ions by amounts ranging from about 5 to 11 kcal mol^{-1}. A molecular orbital picture is proposed that invokes perturbations of π−d donation and d−π* back-donation to explain the particularly unfavorable electronic binding interaction on the concave π face. Binding to the flat coronene π surface is found to be roughly equal to the outside η^5 binding sites of the curved corannulene π surface.

Introduction

The interaction of metal ions with π surfaces, long a central theme of organometallic chemistry, is open to increasingly incisive study by new experimental and computational tools. Flat surfaces from benzene to graphite have often been subject to attention, whereas fullerenes and other curved π surfaces are of more recent but also strong interest. Among the simplest examples of intrinsically curved carbon π systems, corannulene (see Figure 1) is a bowl-shaped C_{20} hydrocarbon whose framework models a portion of the carbon network of C_{60}, as well as other fullerenes and end caps. Its radius of curvature is about 5.3 Å, whereas that of C_{60} is about 3.5 Å. The fact that corannulene is among the simplest of interesting models for the C_{60} surface, along with the recent development of good synthetic access to the molecule,[1] has led to growing interest in metal-ion binding to this molecule. With both accessible convex and concave surfaces, corannulene is a clear-cut model molecule for examining the differences and similarities of metal-binding sites on both types of curved faces.

Recent work from the York group applied advanced experimental and computational techniques to complexation with[2] H^+ and Li^+ and with[3] Fe^+, and their papers provide comprehensive review and referencing of activity in this area, as well as a starting point for the study of more complex systems. The central theme of our interest in this system is the behavior of more complicated metal ions, particularly transition metals, on curved π surfaces. The alkali metal ions provide good benchmarks for understanding the additional effects contributed by the transition-metal d orbitals, so that, as part of the present study, we worked with Na^+ and K^+ (as well as Li^+ with coronene) to extend the careful Li^+ work of Frash et al.[2]

† Part of the special issue "Jack Beauchamp Festschrift".

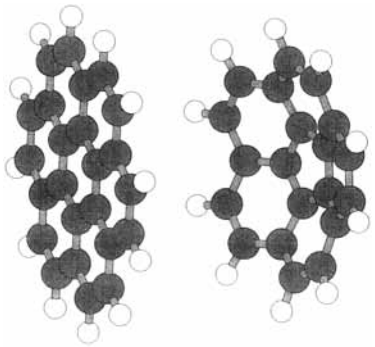

Figure 1. Coronene and corannulene.

Coronene (Figure 1) is close to being a matching, but intrinsically flat, reference hydrocarbon surface for comparison with corannulene. Klippenstein and Yang[4] calculated binding energies of first-row transition-metal ions to coronene at a computational level similar to ours, and the present calculations on the transition-metal−coronene complexes are substantially similar to theirs, aside from our use of a different density functional for consistency with our corannulene results. Our group has observed experimentally the binding of a large variety of metal monocations to coronene,[5] as well as to its isomer tribenzocyclyne,[6] although quantitative binding information is not yet available.

There is active interest in the modes of interaction of metal ions with various sorts of π surfaces. The literature concerning interactions of alkali ions and other closed-shell ions with various π faces is extensive, with research recently stimulated by influential discussions of the relevance of such interactions in biological systems.[7] Gas-phase π binding patterns of more

10.1021/jp020313b CCC: $22.00
Published on Web 08/24/2002

complicated metal ions, and in particular transition-metal ions, have perhaps less obvious biological relevance but are an important focus of recent activity in gas-phase organometallic chemistry in general (see refs 8−10 for surveys.)

Quantitative experimental data for metal−ligand binding energies to π ligands are still sparse and often of limited accuracy and reliability for most metal ions, and in particular, such data are not yet available for extended π systems such as those of interest here. A series of reliable values are known for Na^+ from ligand-exchange equilibrium work[11] and from threshold collision-induced dissociation (TCID)[12,13] for ligands including benzene derivatives. Reliable data for other metal ions are rapidly appearing from experiments using both of these techniques. For transition-metal complexes, the binding energies to benzene measured several years ago by TCID[14] are still highly regarded as benchmarks. A number of bond energies to small aromatic ligands (mainly benzene) have been measured by threshold photodissociation and by other ion-chemistry approaches.[15] Our group measured a series of values for π binding to pyrrole using the radiative association kinetics approach,[16] which gave a periodic trend similar to that found for benzene, and this approach has also been applied to the binding of Cr^+,[17] Au^+,[18,19] and Al^+ [20] to benzene and substituted benzenes.

Metal ions binding to planar π systems tend to favor sites centered over rings (η^5 or η^6 for five- or six-membered rings, respectively). An exception of importance here is Cu^+, for which the η^2 site above the edge of the benzene rings is, at worst, nearly as good as the η^6 central site and might actually be preferred in some cases. For C_{60}, in contrast, the normal site of binding, at least for small metal ions, is the η^2 site over a C−C bond.[21,22] This has been ascribed, at least in part, to the tilting of the p_z orbitals of the rings in C_{60} such that the orbitals are directed unfavorably for binding to the metal ion at either the η^5 or η^6 ring sites. For corannulene, whose curvature is substantially less than that of C_{60}, this effect appears to be less important, and η^5 or η^6 binding on the corannulene surface seems to be normal. The present study is primarily aimed at characterizing the outside/inside differences in binding to curved surfaces and the comparison with flat surfaces, and our focus is on characterizing these effects for the η^5 and η^6 sites. Only a limited exploration of η^2 binding sites is included as an indication that such sites are not favored for most systems of interest here.

It is well-known that the large dipole of corannulene [2.13 D at the B3LYP/6-311G(d,p)//B3LYP/6-31G(d,p) level[2]] points toward the concave side, so that the electrostatic environment of the corannulene bowl is more negative on the outside face than the inside face. For simple, electrostatically interacting cations such as the alkali cations, this factor tends to favor the outside (convex) face for binding. Thus Frash et al.[2] calculated Li^+ to be more strongly bound on the outside than the inside of the bowl (43.9 vs 39.0 kcal mol^{-1} for the on-axis C_5 sites and 44.1 vs 41.1 kcal mol^{-1} for the most stable C_6 sites). On the other hand, alkali ions larger than Li^+, which sit farther from the surface and interact with a larger area of the π surface, should have a polarization interaction that can extend beyond the nearest carbon ring, a factor that might tend to favor binding inside the bowl (concave face) for larger electrostatic ions. For more complex metal ions, and particularly for transition metals, more specific electronic orbital interactions can be expected to play a prominent role, but these effects have yet to be explored.

Most of these questions can only be investigated computationally, because feasible experimental approaches for comparing binding sites are not in prospect. Even if experiments for comparing the C_5 versus C_6 binding sites, for instance, emerge, this will not help in the comparison of inside vs outside binding, because the corannulene bowl inverts very easily[23] and the interconversion of the inside complexes to or from outside complexes is likely to be extremely facile and rapid. Experiment has its major role to play in determining and comparing binding at the most stable site for different metal ions and different ligands: we are pursuing such experimental studies for future comparison with the present computed results.

Computational Methods

The emergence of density functional (DFT) methods has made feasible the computational investigation of transition-metal complexes with relatively large ligands such as those of interest here, and all of the present work was performed with this approach. The alkali cation complexes could perhaps be treated with ab initio methods of potentially greater accuracy, most likely Hartree−Fock/MP2 methods, and this would make an interesting comparison, but the present study used uniform DFT methods for consistency.

The Gaussian 98 program package[24] was employed for all calculations, with the B3LYP, B3P86, and MPW1PW91 functionals. Full geometry optimizations were carried out for all of the investigated structures, with full vibrational frequency analysis for the more important ones to verify that they are true minima on the potential energy surface. The binding energies of all structures were calculated and corrected as described below for zero-point vibrational energy (ZPE) and basis-set-superposition error (BSSE).

Choice of Functionals. The B3LYP hybrid functional has probably been used most often for DFT calculations of transition-metal complexes, but there are some grounds for thinking that the PW91 correlation functional, in particular used as a component of the hybrid MPW1PW91 functional,[25,26] is preferable for transition-metal binding calculations. For example, Porembski and Weisshaar considered the performance of B3LYP to be poor for the energetics of some Y[27] and Zr[28] transition states; they considered the results from MPW1PW91 to be satisfactory and recommended this as the best functional for transition-metal complexes. Zhang et al.[29] considered MPW1PW91 to give better structure results than B3LYP in some Pt complexes. In a recent comparison,[30] MPW1PW91 gave results for benzene complexes of first-row transition metals that agreed slightly better with experiment (although the advantage relative to B3LYP was not dramatic). The present calculations provide another comparison of these two functionals, although the lack of information about the correct binding energies in the present systems precludes any further conclusions about their relative merits.

The MPW1PW91 functional was used here for all transition-metal calculations. For Na^+, the B3P86 hybrid functional has been suggested to agree most closely with existing experimental data[12] and was chosen for the Na^+ work here. For Li^+, where our calculations supplement and extend those of Frash et al.,[2] we used the same B3LYP functional as they did. B3LYP was also used for K^+. A number of comparative calculations for all of the metals were also made using alternative functionals, as described below.

Basis Sets and Optimization. As a standard basis-set protocol, the systems were first geometry-optimized using a basis set of 6-311+g(d) on the metal ion and 6-31g(d) on the carbons and hydrogens. For the final energy calculations of ring-centered sites this basis was augmented with diffuse functions [6-31+g(d)] on the five (or six) carbons comprising the ring

above which the metal ion is bound. For the final energy calculations of η^2 sites, diffuse functions were placed on the seven carbons nearest the metal ion. Various trials have convinced us that, for all of these systems, the addition of the diffuse functions to the carbons has little if any effect on the geometry optimization, although this augmentation is important for the energy calculation and is necessary to bring the BSSE corrections to acceptable magnitudes.

Standard 6-31G(d) and 6-31+G(d) basis sets were used for carbon and hydrogen. For the metal ions, the default 6-311+G(d) basis sets were used. These consist of the standard 6-311+G(d) basis for Li; the Maclean-Chandler[31] basis for Na with default polarization and diffuse functions; the default 6-311+G(d) basis[32] for K; and for the transition metals, the Wachters−Hay[33,34] basis with scaling factors and diffuse functions as recommended by Raghavachari and Trucks.[35]

Geometry optimizations were converged to better than 0.1 kcal mol^{-1}. In most cases, no symmetry was imposed on the structures, even when the optimum structure was expected to be C_{5v}. In those cases where full vibrational analysis was completed, no imaginary frequencies or unreasonably low real frequencies were encountered, and there was nothing to suggest problems with the shape of the potential surface at any of the local minima described here. The η^5 and η^6 metal sites lying over the rings can be stated to be local minima with confidence (except for Cu^+, where the $\eta^2_{hh,out}$ and $\eta^2_{rr,in}$ sites are the stable minima, and K^+, which did not yield a stable η^6 site inside the bowl), because optimization always gave unequivocal, rapid localization of the metal ion to these positions from nearby starting geometries and also because there are no nearby sites of greater stability that could plausibly give rise to saddle points on the potential surfaces.

The η^2 sites for Li^+ are transition states,[2] and for Na^+, a stable η^2 structure was not found at $\eta^2_{hh,out}$ so that this is also a transition state. For K^+, the η^6 and $\eta^2_{hh,out}$ sites are indistinguishably close in energy, and it was not determined whether there is a barrier between them. For Cr^+, the ion did not move away from the $\eta^2_{hh,out}$ site during optimization, and it was not definitively established (by large-basis vibrational calculations) whether this is actually a minimum on the potential surface, although we would guess that it is not. The most stable binding sites of Cu^+ are η^2 sites, as discussed below.

ZPE and BSSE Corrections. It is appropriate to correct the absolute binding energies from such calculations for the overestimation due to the effects of vibrational zero-point energy and basis-set-superposition error. Individual ZPE and BSSE correction calculations are laborious for such large systems; thus, it is interesting to evaluate and, if possible, exploit the use of standard corrections that might be sufficiently accurate and reliable within a particular class of complexes calculated by a consistent computational protocol. The use of standard corrections is attractive for reducing computational effort and can be justified as a reasonable alternative to individual calculations on the basis that the individually calculated corrections show little variation among systems (particularly in the case of ZPE corrections) and have questionable reliability (particularly in the case of BSSE counterpoise corrections).

The use of standard corrections for BSSE seems particularly well justified, because there continues to be serious doubt about whether any counterpoise BSSE calculation provides more than a rough indication of the extent of BSSE effects. Indeed, in a recent cautionary example, Feller[36] found that a counterpoise correction moved Na^+ binding energies to ethylene and benzene farther from the complete-basis-set limit. The point has been made many times that a counterpoise correction is best regarded as an indicator of the magnitude of the possible BSSE effects rather than an accurate compensation for it.

ZPE corrections are more secure in principle, and there is a stronger rationale for calculating them individually wherever possible, but it is doubtful whether the small ZPE variations among the different systems observed here are significant within the computational uncertainty, particularly given the reduced basis set used in the present vibrational calculations. As additional justification for the use of standard corrections in the present work, we can point out that the focus of this work is the comparison of similarly calculated values, for which these errors are largely similar and thus reduced by cancellation.

A variety of sample ZPE and BSSE calculations were made, and standard corrections were applied in the other cases, as follows:

ZPE calculations were made using basis sets of 3-21G(d) on the ligand atoms and 6-311+G(d) on the metal ion. Thirteen specific cases were calculated (nine for corannulene, four for coronene), including at least one for each metal ion and including the most stable structure for each corannulene/metal ion pair. The results were consistent, with no large variation as a function of ligand and differed slightly between alkalis and transition metals. The ZPE corrections averaged 0.8 ± 0.2 kcal mol^{-1} (alkalis) and 0.3 ± 0.2 kcal mol^{-1} (transition metals). For the other structures not specifically calculated, these same values seemed completely justified as standard corrections.

BSSE calculations were made for 15 cases (including the most stable structures for most of the corannulene complexes) with the full basis set, using the geometry-consistent counterpoise approach described by Xantheas.[37] The corrections showed some variation,[38] but consistent patterns appeared: Complexes with the metal ion on the outside of corannulene or on coronene gave corrections of 1.1 ± 0.2 kcal mol^{-1} (alkalis) and 2.0 ± 0.2 (transition metals), whereas complexes with the metal ion inside corannulene were higher than these values by 0.8 kcal mol^{-1}. Following these patterns, standard corrections were applied to the other cases, with the expectation that they would be within 0.5 kcal mol^{-1} of actual counterpoise corrections. We would consider that BSSE problems probably contribute a realistic uncertainty to the absolute binding energies of 1−2 kcal mol^{-1} for the alkalis and 2−4 kcal mol^{-1}for the transition metals at the present level of calculation, not considering additional uncertainties that might arise from basis-set inadequacy, possibly inappropriate choice of functional, and the inexact nature of the DFT approach itself. Thus transition-metal binding energies from calculations such as those presented here should not be regarded as absolutely accurate even within 5 kcal mol^{-1}, although it can be hoped that relative comparisons of the sort considered in the present work would be considerably more reliable.

In the case of the five values for Li^+/corannulene taken from ref 2, we used their uncorrected values and, for consistency, applied the same standard ZPE and BSSE corrections described above. (They apparently did not make a ZPE correction in any case). Judging from the similarity of counterpoise BSSE energies, it appears that their basis and ours are of similar quality, although differing somewhat in detail.

Results

Comparison of Functionals. It seemed of interest to compare the MPW1PW91 functional with the more common B3LYP for some of these systems. Table 1 shows direct comparisons. For corannulene, the most stable binding site was used for these

TABLE 1: Comparison of Different DFT Functionals[a]

	Na^+	K^+	Ti^+	Cr^+	Ni^+	Cu^+
			corannulene			
MPW1PW91	31.7	23.4	65.2	47.1	69.9	61.4
B3LYP	31.7	22.5	60.9	46.0	69.5	61.9
B3P86	30.8					
			coronene			
MPW1PW91	31.6	22.7	55.9	45.1	64.0	58.6
B3LYP	32.0	21.4	50.1[b]	44.8[b]	62.4[b]	57.7[b]
B3P86	30.8					

[a] All outside binding sites are the η^6 site, except that Na^+/corannulene and K^+/corannulene are the η^5 site and Cu^+/corannulene is the η^2 site. Binding energies in kcal mol^{-1}. [b] From ref 4. Because no BSSE correction was made in the original work, we have subtracted 2 kcal from these values for best consistency with the present results.

comparisons, and calculations with both functionals were made using the methodology described above (except that the comparative calculations used the same ZPE and BSSE corrections for all functionals). For coronene, the central binding site was used, and MPW1PW91 results using the present methodology were compared with the B3LYP results from ref 4.

It is seen that the MPW1PW91 functional gave values differing by no more than about 1 kcal mol^{-1} from the B3LYP results except for the early transition metal Ti, for which MPW1PW91 gave binding energies about 5 kcal mol^{-1} higher. These results can be compared with a recent systematic comparison that included the present transition-metal ions binding to benzene and phenol using comparable basis sets.[30] There, it was found that MPW1PW91 gave stronger binding energies than B3LYP for all of the metal ions; for instance, the energy differences between the two functionals were approximately 7 (Ti^+), 2 (Cr^+), 4 (Ni^+), and 2 (Cu^+) kcal mol^{-1}. Comparing these previous observations with the corresponding differences derived from Table 1 in the present work, it is seen that the two functionals are more nearly similar for the present corannulene and coronene cases than they were for the smaller benzene and phenol systems. For corannulene and coronene, the two functionals differed by approximately 1.5 kcal mol^{-1} or less for metals other than Ti^+. This gives rise to the hope that differences between these functionals might be less of a concern for large systems than for ligands of the size of benzene. As expected from the work of Armentrout and Rodgers,[12] B3P86 gave Na^+ binding energies about 1 kcal mol^{-1} less than those obtained with B3LYP.

Computational Results. Table 2 shows the computed results for all of the metal ions considered. In addition to our calculations, results of Frash et al.[2] for Li^+ with corannulene are shown, which were calculated at a comparable level of theory and should be reasonably comparable to our results.

Table 3 gives geometry information for the various sites, and Figures 2−4 display several representative structures, including inside and outside forms and η^5 and η^6 haptomers. The figures include small (Ni^+), medium (Na^+), and large (K^+) ions to give an idea of how the various ions relate to the bowl curvature.

For Ni^+ (Figure 2), the inside η^5 and η^6 sites of corannulene are well separated in space, but for the larger Na^+ ion (Figure 3), these sites are less well separated compared to the ion's distance from the ring. It is not surprising that the larger K^+ ion (Figure 4) does not show separate potential minima for these two possible structures, and we expect that other ions similar to and larger than K^+ will also fill the bowl interior well enough that only a single inside binding site is likely. Outside η^5 and η^6 sites (Figures 2 and 4) were entirely distinct for all cases.

TABLE 2: Calculated Binding Energies of Metal-Binding Sites on π Surfaces (kcal mol^{-1})

		corannulene						
		inside		outside			benzene	coronene
ion	Fn[a]	η^5	η^6	η^5	η^6	η^2	η^6	η^6 (center)
Li^+	B	38.2[b]	39.9[b]	43.0[b]	43.3[b]	38.5[b,c]	38.3	46.6
Na^+	P	27.7	27.4	30.8	29.6	28.1[c]	23.6	30.8
K^+	B	20.6	*c*	22.5	21.3	21.6[c]	14.8	21.6
Ti^+	M	39.4	63.6	53.0	65.2		63.5	55.9
Cr^+	M	38.8	43.2	46.6	47.1	45.4[c]	48.5	45.2
Ni^+	M	52.7	64.4	63.9	69.9		61.3	64.0
Cu^+	M	48.4[d]	55.5[e]	59.7[f]	*c*	61.6[g]	52.7	58.6

[a] Functional used. B = B3LYP, P = B3P86, M = MPW1PW91. [b] Computations of Frash et al.,[2] where we have taken their uncorrected values (before BSSE correction) and applied our standard corrections for BSSE and ZPE effects. [c] Might not be a minimum on the potential surface (see text). [d] For Cu^+, the η^5 site given here is constrained to the symmetry axis of the C_5 ring, which is not a minimum on the potential energy surface. If the ion is allowed to move to the $\eta^2_{hh,in}$ vicinity, the binding energy improves to ~49.1 kcal mol^{-1}, although this is also not a true minimum. [e] No minimum on the potential energy surface was found at the η^6 site over the benzene ring. The energy given is the energy of the peripheral $\eta^2_{rr,in}$ site to which the ion migrates. [f] For Cu^+, the η^5 site given here is constrained to the symmetry axis of the C_5 ring, which is not a minimum on the potential energy surface. [g] This is the $\eta^2_{hh,out}$ site adjacent to the C_5 ring, which was the most stable binding site located.

TABLE 3: Distance from the Metal Ion to the Plane of the Nearest Carbon Ring (Å)

	corannulene					
	inside		outside		benzene	coronene
	η^5	η^6	η^5	η^6	η^6	η^6 (center)
Li^+	1.89[a]	~1.87[a]	1.91[a]	~1.90[a]	1.83	1.80
Na^+	2.40	2.33	2.38	2.34	2.41	2.32
K^+	2.85	−	2.80	2.80	2.82	2.72
Ti^+	2.12	1.81	2.04	1.92	1.88	1.89
Cr^+	2.18	2.13	2.16	2.05	2.09	2.08
Ni^+	1.88	1.66	1.88	1.72	1.93	1.69
Cu^+	1.97[b]	*c*	1.94[b]	*c*	1.84	1.82

[a] Computations of Frash et al.[2] [b] Constrained to symmetry axis of C_5 ring. [c] No minimum on the potential energy surface at this position.

Limited exploration of the possible C_2 (η^2) structures was carried out. Following the notation of Frash et al.,[2] the possible η^2 sites of corannulene are η^2_{hh} (bridging two hub carbons of the five-membered ring), η^2_{hb} (bridging hub to bridgehead carbons), η^2_{br} (bridging bridgehead to rim carbons), and η^2_{rr} (bridging two rim carbons). Because each of these η^2 possibilities can occur either inside or outside the bowl, the possible conformations are numerous and were not examined systematically here. Because $\eta^2_{hh,out}$ is likely to be the most favorable of all of these sites (by analogy with the Li^+ case), several $\eta^2_{hh,out}$ binding energies were calculated as an indication of how the bridging η^2 structures compare with the ring-centered π sites (Table 2). As noted above, we believe that all of these except for Cu^+ are transition states, not local minima on the potential surface.

Discussion

1. Alkali Metal Ions. The steady decrease in binding energies going from Li^+ to Na^+ to K^+ is a straightforward reflection of the increasing size of the ions and consequent lower polarization binding energy. More interesting is the trend of the outside/inside binding-energy differences. Comparing the on-axis η^5 sites, for Li^+, the outside is favored by 5 kcal; for Na^+, by 3

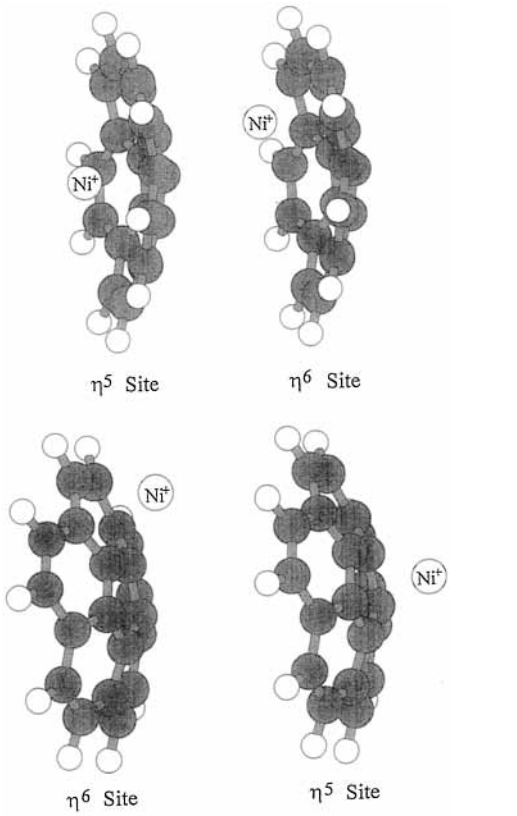

Figure 2. Geometries of Ni^+/corannulene bound to inside and outside sites.

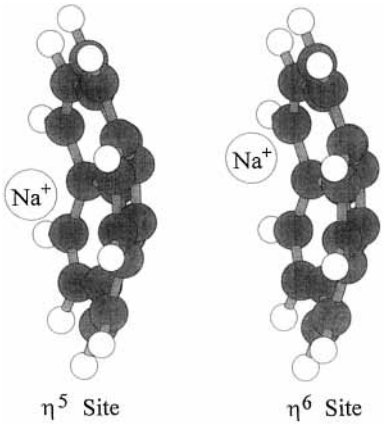

Figure 3. Geometries of Na^+/corannulene inside sites, showing the inside binding site centered on the C_5 ring and that centered on the C_6 ring.

kcal; and for K^+, by only 2 kcal. One argument to rationalize this trend with increasing ion size is that the unfavorable electrostatic potential of the inside region near the five-membered ring becomes weaker as the ion gets farther from the apex and, correspondingly, the favorable potential of the outside region near the apex also drops off with increasing distance.

Comparing corannulene with coronene, it is seen that binding to the outside of the corannulene bowl (at the central η^5 site) is quite similar to binding to coronene. To rationalize this near equality, we can consider two compensating effects: the charge−dipole interaction favors the convex corannulene surface, whereas the polarization interaction favors binding to coronene, both because the flatter surface allows better polarization interaction and also because the metal ion can approach a

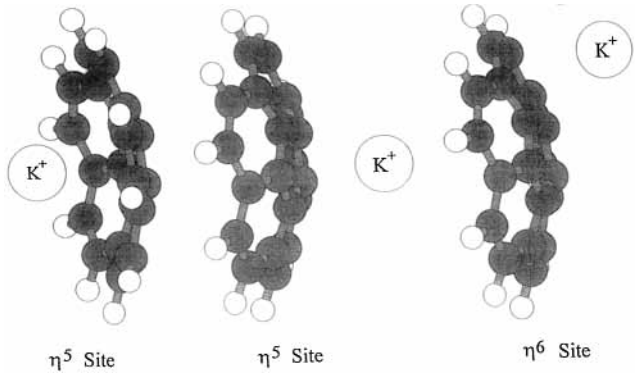

Figure 4. Geometries of K^+/corannulene bound at the inside and outside sites.

bit closer to the plane of the six-membered ring than the five-membered ring (Table 3). These two opposite effects appear to compensate to give equal binding.

Frash et al.[2] found the η^6 sites to be somewhat favored over the η^5 sites for Li^+, but this tendency does not seem to hold for the larger alkalis. For Na^+ and K^+, the η^5 sites of corannulene are about equal to the corresponding η^6 sites, or even slightly favored (although the differences are so small that we would not place much confidence in saying that they are actually favored). For K^+ inside the bowl, the putative η^5 and η^6 sites would be very close in space, so that their separate existence would be doubtful. Attempts to place K^+ over the C_6 ring resulted in optimization to the stable η^5 site over the C_5 ring.

Alkali binding to the simple benzene ligand (shown at the same computational level for comparison in Table 2) is substantially weaker than binding to the more extended π faces of this study. Even the least favorable corannulene surface sites are significantly stronger than those of benzene. This is a reflection of the greater polarization interaction with the more extended π surfaces, in comparison with those of the small benzene ligand.

The coronene face is a model for the flat, featureless graphite basal plane. To the extent that the coronene surface is a faithful model of the infinite planar surface, we expect the different η^6 π sites on this surface to be equivalent. Thus, it was interesting to investigate whether a surface-bound ion has a preference for one or the other of the two types of η^6 π sites of coronene. This was tested for Na^+. It was found that Na^+ binds over the peripheral benzene rings exactly as well as it does over the central benzene ring: these binding energies were found the same to within 0.1 kcal mol^{-1}.

The $\eta^2_{hh,out}$ corannulene sites of Li^+ [2] and Na^+ are less stable than the adjacent η^5 and η^6 sites, but as we progress to the larger K^+ ion, all of the various sites become close in energy. For large alkalis, it is probably best to consider the π surface as approximately smooth, with an overall tendency for the ion to move to the minimum on the potential energy surface at the outside apex of the bowl.

2. Transition-Metal Ions. Table 2 immediately shows that outside/inside differences are much larger for the transition metals than for the alkalis at the on-axis η^5 sites. As discussed below, this is interesting to the extent that these apex sites can be considered as models for binding to curved carbonaceous surfaces. It is obvious that, in addition to the electrostatic[39] and polarization effects operating for the alkalis, there are electronic orbital effects at work to give a large additional stabilization of the convex face relative to the concave face. However, considering the η^6 sites (which represent the most stable binding positions in most cases), it is seen that the inside/outside

differences tend to be smaller and that there is little distinction between alkalis and transition metals in this respect.

For cases of similar ion size, the first-row transition metals bind much more strongly than the alkalis to π faces. A particularly clear example is the comparison of Li^+ and Ni^+, which have virtually identical binding geometries but binding energies that differ by 15−26 kcal for the various sites (Tables 2 and 3).

A striking observation for the transition metals is the large difference in the outside vs inside binding energies for the central η^5 sites, with binding on the convex (outside) face being much better than that on the concave (inside) face. This is interesting to the extent that it might reflect a general property of binding to curved carbon surfaces. The next section addresses the possibility that this difference might be largely a reflection of the different electrostatic environments or different local polarizability properties of the two sides of the bowl; it is concluded that these factors are much less than the observed differentials and, moreover, are not distinctive for the transition metals as compared with the alkalis. Section 4 outlines an electronic orbital argument that might provide an understanding of this distinctive characteristic of transition-metal binding.

The results for the η^6 sites (the peripheral benzene rings of corannulene) do not lead to such clear generalizations. In each case, the η^6 site is more stable than the neighboring η^5 site, by varying amounts. The inside η^6 sites are less favorable than the corresponding outside sites, but these differences are fairly small, nothing like the large differentials seen for the η^5 sites. Although a semiquantitative analysis along the lines of section 3 was not attempted for sites other than the central η^5 sites, it seems likely that the modest outside/inside differentials found for the η^6 sites can be accounted for largely by electrostatic and polarization effects, without the need to consider important electronic orbital effects. Our conclusion is that there are distinctively unfavorable effects at work when a transition-metal ion is bound at the inside η^5 position right in the middle of the bowl, but that these effects cease to be as important when the metal ion moves to the peripheral inside η^6 position over a benzene ring and are also not as important anywhere on the outside of the bowl.

Comparing corannulene binding (at the favored η^6 benzene-ring sites) with binding to benzene itself, the alkalis serve as models to show that the ordinary electrostatic and polarization effects strengthen binding to corannulene by perhaps 6 kcal mol^{-1} at the favored outside sites. With so few transition-metal examples, conclusions on this point can only be speculative, but it appears that the early transition-metal ions Ti^+ and Cr^+ are slightly less strongly bound to corannulene than their benzene binding values would predict, whereas the late metals Ni^+ and Cu^+ are bound slightly more strongly than would be expected. These effects might perhaps be rationalized by extending the arguments of section 4 below, but this would be highly speculative.

Calculations were successful for some η^2 sites of Cr^+ and Cu^+. Cr^+ gave straightforward results, with the $\eta^2_{hh,out}$ site having a binding energy 1−2 kcal mol^{-1} less than that of the adjoining ring-centered sites. Cu^+ was less straightforward. None of the η^5 or η^6 ring-centered sites was a minimum on the potential energy surface, and the ion always migrated to a nearby edge. Some η^2 sites were local minima, but both the inside $\eta^2_{hh,in}$ site and the outside $\eta^2_{rr,out}$ site were unstable. A Cu^+ ion placed at the inside apex of the bowl migrated steadily outward all the way to the periphery, ending at $\eta^2_{rr,in}$. An ion placed on the outside periphery migrated inward to the central $\eta^2_{hh,out}$ site. Data in Table 2 suggest that the edge-bound η^2 sites for Cu^+ are generally about 2 kcal mol^{-1} more stable than nearby ring-centered locations. This parallels the behavior of Cu^+ found for both phenol[30] and pyrrole[16] π binding, where migration to the edge of the ring gave an energy improvement relative to the central region of the ring. For benzene itself, Cu^+ π binding seems to prefer the central η^6 location,[40] but edge binding is nearly equally good.[30] Finally, for Ni^+, η^2 calculations did not succeed, but the η^5 ring-centered location was definitely a local minimum on the potential energy surface, so that an ion placed near the η^5 ring center moved back to the central position. Attention is focused in the following discussion on the ring-centered binding sites because the η^2 sites appear, in most cases, to be slightly less stable than nearby ring-centered sites and, even in the Cu^+ cases where η^2 binding is slightly favored, the ring-centered locations are stable enough for their binding to be interesting.

Previous coronene calculations have considered η^6 binding to be likely. If this assumption is actually incorrect, the most likely one of these metal ions to favor η^2 binding would be Cu^+, so a check was made with the present protocols to test the possibility of η^2 binding in Cu^+/coronene. The interior C_2 site (η^2_{hh} in the same terminology as used for corannulene) was found to be a stable local minimum on the potential energy surface for this complex, in the sense that the ion optimized to this site from nearby locations. However, this site was 2.7 kcal mol^{-1} less stable than the central η^6 binding site for the same ion. We conclude that η^2 binding on coronene is unlikely to be favored for any of the metal ions examined.

Interestingly, the peripheral η^6 site of coronene was found to be more stable than the central η^6 site by 1.6 kcal mol^{-1} for Cr^+ and by 2.0 kcal mol^{-1} for Cu^+ (in contrast to the Na^+ case where they were equal.) These differences are small, but they lead us to surmise that the central site of coronene is not quite the best binding site for transition metals and that the central-site binding energies calculated here and in ref 4 are probably slightly lower (by 1 or 2 kcal mol^{-1}) than the best sites for transition-metal/coronene complexes.

3. Analysis of Electrostatic and Polarization Contributions. One of the aims of the present work was to characterize the effect of curvature of the carbonaceous surface on metal ion binding using corannulene as a model. Although the calculations show clearly that the strongest binding to corannulene in some cases is on the benzene-ring sites, it is nevertheless interesting to clarify binding to the central η^5 positions on the inside and outside of the corannulene bowl, considering that these sites provide relevant models of curved-surface binding in general. The best quantitative understanding of these effects must be drawn from the quantum calculations themselves, but a low-order semiquantitative model is useful as a first approach to clarifying the various contributions to the binding. In particular, the large outside/inside differences in binding of the transition-metal ions, contrasted with that of the alkalis, suggest large electronic-orbital effects at work, and it is interesting to try to dissect the binding in these systems in such a way as to identify such contributions.

We can picture the binding to be composed of four main components

$$E_{bind} = E_{es} + E_{polariz} + E_{orbital} - E_{repuls} \qquad (1)$$

Here, E_{es} is the binding energy of the ion charge in the electrostatic potential field of the molecule,[39] $E_{polariz}$ is the binding energy due to polarization of the neutral by the ion charge, $E_{orbital}$ is the specific electronic orbital interactions, and

TABLE 4: Binding to the Central η^5 Sites of Corannulene, Analyzed in Terms of a Sum of Ionic and Orbital Contributions (kcal mol^{-1})[a]

	η^5 inside			η^5 ouside		
ion	E_{ionic}	E_{total}	$E_{orbital}$	E_{ionic}	E_{total}	$E_{orbital}$
Li^+	52.7	38.2	0.2	59.5	43.0	0.0
Na^+	35.7	27.7	2.7	42.0	30.8	0.6
K^+	25.8	20.6	2.7	30.8	22.5	0.4
Ti^+	47.5	39.4	7.1	55.1	53.0	18.3
Cr^+	45.3	38.8	8.4	50.5	46.6	14.0
Ni^+	56.9	52.7	16.1	61.6	63.9	26.9
Cu^+	53.2	48.4	13.8	59.0	59.7	23.7

[a] E_{ionic} is the binding energy contribution to the η^5 complex calculated by the DFT point-charge approach, E_{total} is the total dft binding energy (from Table 2), and $E_{orbital}$ is ($1.385E_{total} - E_{ionic}$), as derived in the text.

E_{repuls} is the short-range repulsion energy between the ion and the neutral. The goal of the present analysis is to make realistic estimates of the components contributing to this energy and to compare these estimates with the total binding energy from the full quantum DFT calculations.

Estimating E_{ionic}. The classical binding energy due to ionic interactions is the sum $E_{ionic} = (E_{es} + E_{polariz})$. The approaches frequently used to model E_{es} and $E_{polariz}$ for simpler systems are not very satisfactory for our purposes. E_{es} has often been estimated by a classical charge−multipole interaction, typically limited to the leading nonzero term (which is the charge−dipole or the charge−quadrupole interaction, depending on whether the molecule has a permanent dipole). At a similar level of consideration, $E_{polariz}$ has often been estimated by the interaction energy of a point charge with a sphere of polarizable material having the same polarizability as the actual molecule. Neither of these long-range approximations is likely to be useful for estimating the interaction energy of a metal ion with a highly extended molecule such as corannulene lying at a distance from the metal ion that is small compared with the dimensions of the molecule. The charge−multipole expansion for E_{es} performs poorly, because short-range terms higher than dipole or quadrupole terms are far from negligible. Similarly, the charge−induced-dipole description of $E_{polariz}$ using the overall molecular polarizability is poor when the charge is close to the extended molecule. It might be possible to improve these approaches with, for instance, distributed multipole and distributed polarizability formulations,[41] but this was not attempted here.

Although such approximate classical approaches to E_{es} and $E_{polariz}$ thus have doubtful utility for the present purpose, it is straightforward to make quite a good estimate of E_{ionic} by an alternative quantum computational approach. In this approach, the metal ion is replaced by a point charge at the same location, and the calculated energy of this system is compared with the corresponding calculation performed with the point charge removed to an infinite distance. This calculation automatically includes both E_{es} and $E_{polariz}$ while excluding all of the electronic-interaction contributions. This approach was carried out for the inside and outside η^5 sites of all of the corannulene complexes using the same level of theory and the same basis sets as the calculations reported in Table 2. The results are displayed in the E_{ionic} column of Table 4.

We can note that it is also possible to determine E_{es} directly with quantum calculations. Klarner et al.[42] surveyed the inside and outside environments of aromatic bowls in this way, concluding that, in general, DFT methods give a more negative electrostatic environment inside the bowl than outside. However, we carried out electrostatic mapping of the corannulene system at the level of calculation of the present study and found that, in the regions of C_5 ring-centered binding, the outside is more negative than the inside (as suggested by the direction of the dipole moment). The situation is more complex as one moves away from the axis, and there are off-axis regions where the inside becomes electrostatically significantly negative. Because E_{es} is much less useful for our purposes than E_{ionic}, this line of investigation was not pursued further.

Estimating E_{repuls}. The contribution of E_{repuls} is harder to estimate. Recognizing that it is a highly approximate approach, the following analysis can lead to useful first approximations. Assume the ion−ligand interaction energy to be composed of long-range attractive components and short-range repulsive components with the functional form

$$V(R) = V_{attraction} + V_{repulsion} = -AR^{-n} + BR^{-12} \qquad (2)$$

where A and B are positive parameters whose actual values will not matter here and R is an appropriate measure of the distance between the ion and the ligand. The exponent n governing the attractive interaction is quite uncertain and is to be considered as an empirical parameter combining the various attractive forces. Attractive forces can be considered to include terms having n values ranging from 2 (ion−dipole electrostatic interactions) to 3 (ion−quadrupole interactions) to 4 (polarization interactions) to around 6 (short-range attractions). The assignment of an overall value of n is empirical, with the presumption that the appropriate value lies somewhere between 2 and 6. As will be seen, there is some justification for using n near 3.3 in the present cases.

At the equilibrium binding distance R_o, the condition is that

$$\frac{dV}{dR} = 0$$

which leads immediately to

$$V_{repulsion}(R_o) = -\frac{n}{12}V_{attraction}(R_o) \qquad (3)$$

This equation forms a basis for making first-order estimates of the repulsion energies. This approach provides a useful approximation as long as n is much less than 12, so that the repulsive force falls off much more steeply than the attractive force rises, and it becomes accurate in the hard-sphere limit where the repulsive wall is vertical.

Estimating $E_{orbital}$. Making a correspondence of $V_{repulsion}$ (eq 3) with E_{repuls} (eq 1) and a correspondence of $V_{attraction}$ with the remaining terms on the right of eq 1, eq 3 can be substituted into eq 1 and rearranged to give an estimate of $E_{orbital}$ as

$$E_{orbital} = \left(\frac{1}{1 - (n/12)}\right)E_{total} - E_{ionic} \qquad (4)$$

To apply this result, we take E_{total} from the binding energy calculated by the full DFT calculation and E_{ionic} from the DFT point-charge model calculation. Depending on the value assigned to n (between 2 and 6), the resulting estimates of $E_{orbital}$ can vary over a considerable range. A criterion for narrowing this choice is to require that the estimated orbital contributions be small for alkali ion binding, which is usually considered to be nearly pure ionic binding. Imposing this condition on the outside binding site of Li^+ leads to a value of n near 3.3, which seems very reasonable. The resulting decomposition of the binding into ionic and orbital contributions is shown in Table 4 for the η^5 corannulene sites. The model is apparently successful in the

TABLE 5: Outside/Inside Binding Energy Differential on Corannulene, Analyzed in Terms of a Sum of Ionic, Short-Range Repulsive, and Electronic Orbital Contributions[a,b]

ion	ΔE_{total}	ΔE_{ionic}	ΔE_{repuls}	$\Delta E_{orbital}$
Li^+	4.8	6.8	1.8	−0.2
Na^+	3.1	6.3	1.1	−2.1
K^+	1.9	5.0	0.8	−2.3
Ti^+	13.6	7.6	5.2	11.2
Cr^+	7.7	5.1	3.0	5.6
Ni^+	11.2	4.6	4.2	10.8
Cu^+	11.1	5.9	4.7	9.9

[a] Values given are the difference de between outside and inside h5 conformations of the corannulene complexes (kcal mol^{-1}). [b] ΔE_{total} is the total outside/inside binding energy differential from the dft results, ΔE_{ionic} is the energy differential modeled by the point-charge−ligand interaction, ΔE_{repuls} Is the differential of the short-range repulsion contributions, and $\Delta E_{orbital}$ is $(1.385\Delta E_{total} - \Delta E_{ionic})$.

sense that all of the estimated $E_{orbital}$ contributions for the alkalis are small, whereas the orbital contributions for the transition-metal ions are substantial.

Outside/Inside Comparison: The decomposition of binding into ionic attractions, short-range repulsions, and electronic orbital attractive interactions just described is highly approximate and should not be taken too far. However, many of the uncertain features can be hoped to cancel in making comparisons between the outside and the inside of the corannulene bowl for a given metal ion. The outside/inside difference of binding energies will be designated ΔE_{total}, with similar definitions of the other difference quantities. Following eqs 1 and 4 and using a value of 3.33 for *n*, we can write

$$\Delta E_{total} \equiv E_{bind}(\text{outside}) - E_{bind}(\text{inside}) = \Delta E_{ionic} + \Delta E_{orbital} - \Delta E_{repuls} \quad (5)$$

$$\Delta E_{orbital} \approx 1.385\Delta E_{total} - \Delta E_{ionic}. \quad (6)$$

The modeling approach consists of assuming that the point-charge DFT model calculations give a useful approximation for the ΔE_{ionic} component and that the approach outlined above for ΔE_{repuls} gives a reasonable estimate of the outside/inside differential repulsion energy. This simple analysis should give an idea of the relative contributions of ionic and orbital effects acting on the convex and concave π surfaces. We expect $\Delta E_{orbital}$ to be small for the alkalis. Testing this expectation gives a check on the validity of this way of viewing the binding. For the transition metals, $\Delta E_{orbital}$ can give some indication of the importance of electronic orbital effects acting in addition to ΔE_{ionic} effects.

Table 5 shows the results of these calculations. The second column of Table 5 gives ΔE_{ionic} as approximated by the point-charge DFT calculations, and the third column gives the accurate calculations of ΔE_{total} as calculated from Table 2. The last column of the table, giving the estimates of $\Delta E_{orbital}$ from eq 6, is the final result of this modeling procedure. The small deviations of $\Delta E_{orbital}$ from zero found for the alkalis are not unreasonable within such an approximate model. For the transition-metal ions the $\Delta E_{orbital}$ results indicate major contributions of orbital interaction effects to the outside/inside differential, with $\Delta E_{orbital}$ estimates ranging from about 5 to 11 kcal mol^{-1}. For Cr^+, $\Delta E_{orbital}$ is smaller than for the others. This accords with the fact that this ion, with its filled half-shell of d electrons, binds relatively weakly to aromatic faces in general. The other transition-metal ions exhibit larger contributions of electronic orbital binding effects to ΔE_{total}. The next section outlines one line of reasoning that can explain this prominent difference in binding behavior of the transition metals compared with the alkalis.

4. Molecular Orbital Analysis. A notable feature of these results is the strong outside/inside differential for the transition metals, which was dissected in the preceding section to give quite large estimates of $\Delta E_{orbital}$ for the transition-metal ions. A molecular orbital argument can help to explain this disfavoring of the concave face of corannulene and might be applicable to a wider range of curved π faces. The favorable interaction of transition metals with π cycles is commonly attributed to a combination of electron donation from occupied π orbitals into unoccupied metal d orbitals and back-donation from occupied metal d orbitals into low-lying unoccupied π^* orbitals of the ligand. Both π donation and π^* back-donation stabilization effects depend on the occupation situation of the metal d orbitals, which leads to a strong modulation of the binding energies across the periodic table. These ideas go far toward rationalizing the periodic trend in the binding of transition-metal ions to ligands such as benzene[40] and pyrrole.[16]

For small π monocycles such as benzene, the lowest unoccupied molecular orbital (LUMO), or at least one of the lowest-lying unoccupied π^* orbitals, has the same symmetry as the d_{xy} or $d_{x^2-y^2}$ orbitals of the metal, making back-donation favorable for metal ions in which one or both of these d orbitals are occupied. Moreover, the highest occupied ligand π molecular orbital (HOMO) has the same symmetry as the d_{xz} or d_{yz} orbitals, allowing orbital overlap corresponding to π donation when there are vacancies in these metal orbitals. To carry this picture on to more extended π systems, we describe the situation for the d−π^* back-donation interaction to consider how the interaction is modified in the case of extended, curved π surfaces. At the end, we point out that the same argument applies in the same way to the effects of curvature on the π−d donation interaction.

The following discussion develops our picture of π binding effects in extended, curved π surfaces by making two key observations: First, in extended π systems (corannulene and coronene here), the low-lying unoccupied ligand orbitals having the correct symmetry for back-donation interactions with the metal ion are less favorable for d/π^* overlap than in the case of the monocycles such as benzene. Second, this disfavoring of back-donation interaction is much more severe for a metal ion on the concave face than for one on the convex face.

A degenerate pair of low-lying unoccupied π^* orbitals of corannulene with the appropriate shape to overlap with a metal $d_{x^2-y^2}$ or d_{xy} orbital exists. One of these virtual orbitals is shown in Figure 5. The shape of this π^* orbital above the inner (C_5) carbon ring is similar to the acceptor π^* orbital of benzene which gives the back-donation overlap in the benzene situation. [Note that this orbital approximates four-fold (S_4) symmetry, despite the five-fold axis of the carbon framework.] However, this orbital also has a major contribution from the p_z orbitals of the carbons comprising the outer carbon ring, and this contribution is seen to have a reversed phase relative to the inner ring; thus, this outer portion of the orbital will act against the formation of overlap with the metal d_{xy} orbital. This idea is illustrated again from a different perspective in Figure 6, showing side-view cross sections through the orbitals. Figure 6a shows the cross section of the same π^* orbital as shown in Figure 5, while parts b and c of Figure 6 show schematically the overlap of this orbital with a metal d_{xy} orbital. (In this illustration, the metal ion is positioned as in the Ti^+/corannulene complex, and the d_{xy} orbital is that of Ti^+.) These diagrams illustrate how the out-of-phase outer lobes of the π^* orbital of

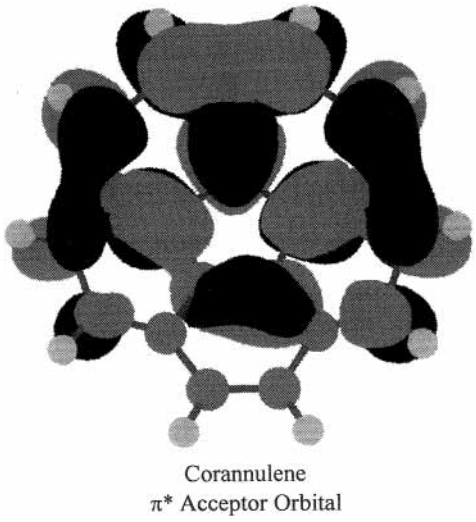

Figure 5. One of the pair of degenerate low-lying π^* virtual orbitals of corannulene having appropriate geometry to overlap with occupied Ti^+ $d_{x^2-y^2}$ and d_{xy} orbitals. (Note that the *z* axis lies along the C_5 symmetry axis.)

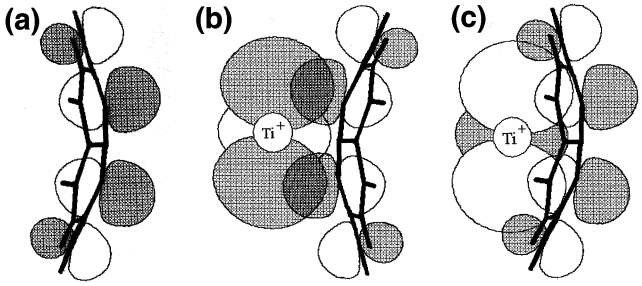

Figure 6. Cross-sectional view of molecular orbitals involved in d−π^* back-donation: (a) cross section of the same molecular orbital of corannulene as shown in Figure 5; (b,c) same view, with a superimposed cross section of the metal d_{xy} orbital of Ti^+ placed at the outside or inside η^5 binding positions, respectively. (The *z* axis lies along the C_5 symmetry axis.)

corannulene are positioned so as to give negative overlap with the metal orbital. Furthermore, it is clear that this unfavorable contribution to the overlap is much more severe for the inside complex than the outside one (compare parts b and c of Figure 6). Finally, Figure 7 shows the resulting molecular orbital of the Ti^+/corannulene complexes that derives from the perturbed d_{xy} metal orbital. This orbital is occupied in the metal ion, and the extent to which its electron density moves toward the ligand upon complexation is a reflection of the extent of the back-donation electronic effect. In this figure, it is seen that the outside complex (Figure 7a) has a noticeable shift of electron density toward the corannulene ring (reflecting a degree of back-donation in this complex), whereas the inside complex (Figure 7b) has a metal orbital almost entirely unchanged by the proximity of the ligand, reflecting little back-donation interaction in this case.

This argument has been developed using one of the pair of degenerate π^* orbitals interacting with the metal d_{xy} orbital for illustration. An exactly parallel situation exists for the other member of the π^* orbital pair, whose interaction is with the metal $d_{x^2-y^2}$ orbital. Whether one or both of these interactions operates in a given complex depends on the occupancy of the metal d_{xy} and $d_{x^2-y^2}$ orbitals, but either or both of these effects will operate in such a way as to reduce the d−π^* back-donation.

A similar situation is obtained for the metal ion sitting over the central ring of coronene. Again in this case, the d−π^* back-donation is inhibited by the out-of-phase contribution to the π^* orbital from the peripheral carbons of the coronene system. However, the extent of unfavorable overlap in this case is relatively small, probably comparable to that in the outside corannulene complexes. This gives a partial rationalization for the observation that the coronene complexes and the corresponding outside corannulene complexes tend to have fairly similar binding energies.

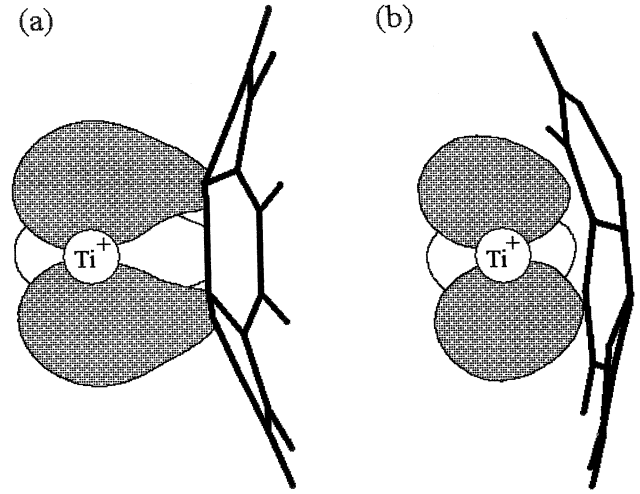

Figure 7. Occupied molecular orbital derived from the metal-ion d_{xy} orbital of the (a) outside and (b) inside η^5 complexes of Ti^+ with corannulene. (The *z* axis lies along the C_5 symmetry axis.)

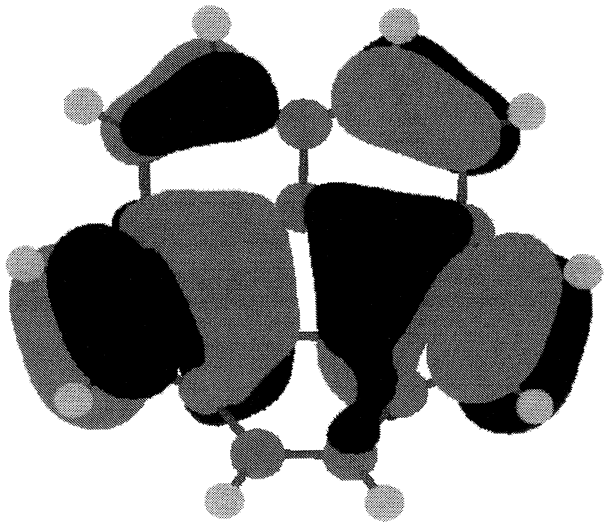

Figure 8. One of the pair of degenerate occupied π orbitals of corannulene having appropriate geometry to overlap with unoccupied Ti^+ d_{xz} and d_{yz} orbitals. (The *z* axis lies along the C_5 symmetry axis.)

We have developed in detail the qualitative picture of suppression of d−π^* back-donation in extended π systems. It can be pointed out finally that the argument is precisely the same with regard to the binding interaction arising from π−d donation. To make this fact clear, Figure 8 displays one of the pair of occupied molecular orbitals of corannulene that has the appropriate symmetry to overlap with a metal d_{xz} or d_{yz} orbital and, thus, to participate in π−d donation. Just as with the ligand π^* orbital discussed above, it is seen that the extended π system of coronene contributes oppositely phased lobes of wave function amplitude lying outside the central region. Just as was discussed above, these wrongly phased lobes can be pictured

as decreasing the overlap with the metal d orbitals, thereby tending to suppress the $\pi-$d donation. Moreover, this effect will again be much more severe for a metal ion inside a concave face than for one outside the convex face (as in the comparison of parts b and c of Figure 6). Thus, the perturbations of d$-\pi^*$ back-donation and of $\pi-$d donation lead in precisely the same way to an expected disfavoring of transition-metal π binding for extended π surfaces and particularly for concave π surfaces.

The mild preference of Cr^+ and Cu^+ for binding to sites on the peripheral rings of coronene rather than the site over the central ring might be another reflection of this molecular orbital effect. A metal ion sitting over the peripheral ring will not be completely surrounded by the ring of unfavorably phased carbon p_z orbitals that are postulated to diminish d$-\pi$ interactions. Although this mechanism might operate to give some reduction of binding interactions at peripheral π sites, it should be less important than for central π sites.

It has been suggested that the relatively poor outside η^6 face binding of transition metals to C_{60} (relative to η^2 edge binding) might be due to the outward-tilted geometry of the carbon p_z orbitals, with consequently reduced overlap of the π and π^* orbitals with the metal orbitals, and, further, that this situation might be improved by using larger metals.[21] The tilted-orbital argument has been extended to apply as well to the disfavoring of η^5 coordination to corannulene.[3] Note that these authors have considered that the outward tilting of the π orbitals on the outside π faces acts to *reduce* the binding energy.

The present results suggest that this argument is, at the least, not the whole story. This tilted-orbital argument should apply more strongly to the transition-metal cases than to the alkalis, because π/d overlap characteristics are much more important for the transition metals, whereas π/s overlap in the alkali case is not considered to play a major role in the binding interaction. It is indeed seen from Table 1 that the transition metals Cr^+ and Cu^+ are slightly more favorable to η^2 edge binding than the alkalis as predicted by this picture. However, this line of reasoning also leads to a prediction of enhancement of inside versus outside binding for the transition metals (because the tilt of the carbon p_z orbitals is favorable to π/d overlap inside the bowl). Contrary to this expectation, the outside/inside comparisons discussed in connection with Table 5 above show that the electronic effects of orbital interactions actually favor outside binding strongly over inside binding for the transition-metal ions, a result that is completely unexplained by orbital tilting. Thus, orbital-tilting effects might be operative in these systems, but other important electronic orbital effects that do not correspond to the orbital-tilt picture are also operating. This motivates our proposal of the suppression of $\pi-$d donation and d$-\pi^*$ back-donation as described here.

Conclusions

The curvature of the π surface exerts a major effect on the binding of transition-metal ions. For a given metal on corannulene, outside binding to the C_5 ring site on of the order of 10 kcal mol^{-1} stronger than binding to the corresponding inside site. For the C_6 sites, the outside/inside differential is less, but it still averages 4 kcal mol^{-1}. Some of this differential certainly arises from the well-known interaction of the charge with the corannulene dipole field. However, a comparison of these effects with those for alkali metal ions suggests that much of the observed differential arises from the specific electronic interactions of the transition metals. The point-charge modeling described in section 3 of the Discussion lends semiquantitative support to this assignment of the outside/inside differentials in large part to electronic orbital interactions of the transition metals. A molecular orbital mechanism that reduces both $\pi-$d donation and d$-\pi^*$ back-donation in the concave extended π system is described and suggested as a rationalization for this effect of the surface curvature. The same effect is expected to operate to a lesser extent with coronene, and it might rationalize the surprising calculated result that coronene binds less strongly than benzene to the two transition metals (Ti^+ and Cr^+) with the largest d orbitals among the metals considered here.

Binding to the flat coronene surface is approximately equal in strength to binding to the convex C_5 face of corannulene. We can speculate that this reflects a balance of the charge$-$dipole interaction favoring binding to corannulene with the polarization effects favoring binding to coronene. Binding to the convex C_6 site of corannulene is similar to binding to the convex C_5 site (and similar to coronene) for most of the ions, but it is substantially stronger for Ni^+ and Ti^+. Moreover, the concave C_5 site for these two metal ions is also exceptionally weakly bound compared with the concave C_6 site, a result that gives support to the molecular orbital argument provided here for destabilization of the concave C_5 site.

This computational approach should not be expected to provided highly accurate absolute binding energies for these systems, although the estimates given should be useful for experiment planning. The relative values should be more reliable, and we conclude with confidence that the concave face of corannulene is less favorable for binding than the convex face and that this differential is much more pronounced for the transition metals than for the alkalis. Whether this situation might reverse for larger ions remains to be investigated.

Acknowledgment. The support of the donors of the Petroleum Research Fund, administered by the American Chemical Society, and of the Ohio Supercomputer Center is gratefully acknowledged. This work is dedicated to Jack Beauchamp on the occasion of his 60th birthday in tribute of and with gratitude for his personal and scientific leadership over the years.

References and Notes

(1) Sygula, A.; Rabideau, P. W. *J. Am. Chem. Soc.* **2000**, *122*, 6323.
(2) Frash, M. V.; Hopkinson, A. C.; Bohme, D. K. *J. Am. Chem. Soc.* **2001**, *123*, 6687.
(3) Caraimon, D.; Koyanagi, G. K.; Scott, L. T.; Preda, D. V.; Bohme, D. K. *J. Am. Chem. Soc.* **2001**, *123*, 8573.
(4) Klippenstein, S. J.; Yang, C. N. *Int. J. Mass Spectrom.* **2000**, *201*, 253.
(5) Pozniak, B. P.; Dunbar, R. C. *J. Am. Chem. Soc.* **1997**, *119*, 10439.
(6) Dunbar, R. C.; Uechi, G. T.; Solooki, D.; Tessier, C. A.; Youngs, W.; Asamoto, B. *J. Am. Chem. Soc.* **1993**, *115*, 12477.
(7) Ma, J. C.; Dougherty, D. A. *Chem. Rev.* **1997**, *97*, 1303.
(8) Fisher, K. J. *Prog. Inorg. Chem.* **2001**, *50*, 343.
(9) *Organometallic Ion Chemistry*; Freiser, B. S., Ed.; Kluwer Academic Publishers: Dordrecht, The Netherlands, 1996.
(10) Rodgers, M. T.; Armentrout, P. B. *Mass Spectrom. Rev.* **2000**, *19*, 215−247.
(11) Hoyau, S.; Norrman, K.; McMahon, T. B.; Ohanessian, G. *J. Am. Chem. Soc.* **1999**, *121*, 8864.
(12) Armentrout, P. B.; Rodgers, M. T. *J. Phys. Chem. A* **2000**, *104*, 2238.
(13) Amicangelo, J. C.; Armentrout, P. B. *Int. J. Mass Spectrom.* **2001**, *212*, 301.
(14) Meyer, F.; Khan, F. A.; Armentrout, P. B. *J. Am. Chem. Soc.* **1995**, *117*, 9740.
(15) Ranasinghe, Y. A.; Sujasasmita, I. B.; Freiser, B. S. Gas-Phase Organometallic Ion Photochemistry. In *Organometallic Ion Chemistry*; Freiser, B. S., Ed.; Kluwer Academic Publishers: Dordrecht, The Netherlands, 1996.
(16) Gapeev, A.; Yang, C.-N.; Klippenstein, S. J.; Dunbar, R. C. *J. Phys. Chem. A* **2000**, *104*, 3246.
(17) Lin, C.-Y.; Dunbar, R. C. *Organometallics* **1997**, *16*, 2691.

(18) Ho, Y.-P.; Dunbar, R. C. *Int. J. Mass Spectrom.* **1999**, *182/183*, 175.
(19) Schröder, D.; Brown, R.; Schwerdtfeger, P.; Schwarz, H. *Int. J. Mass Spectrom.* **2000**, *203*, 155.
(20) Dunbar, R. C.; Klippenstein, S. J.; Hrušàk, J.; Stöckigt, D.; Schwarz, H. *J. Am. Chem. Soc.* **1996**, *118*, 5277.
(21) Rogers, J. R.; Marynick, D. S. *Chem. Phys. Lett.* **1993**, *205*, 197.
(22) Fujimoto, H.; Nakao, Y.; Fukui, K. *J. Mol. Struct.* **1993**, *300*, 425.
(23) Sastry, G. N.; Priyakumar, U. D. *J. Chem. Soc., Perkin Trans. 2* **2001**, *2*, 30.
(24) Frisch, M. J.; Trucks, G. W.; Schlegel, H. B.; Scuseria, G. E.; Robb, M. A.; Cheeseman, J. R.; Zakrzewski, V. G.; Montgomery, J. A. Jr.; Stratmann, R. E.; Burant, J. C.; Dapprich, S.; Millam, J. M.; Daniels, A. D.; Kudin, K. N.; Strain, M. C.; Farkas, O.; Tomasi, J.; Barone, V.; Cossi, M.; Cammi, R.; Mennucci, B.; Pomelli, C.; Adamo, C.; Clifford, S.; Ochterski, J.; Petersson, G. A.; Ayala, P. Y.; Cui, Q.; Morokuma, K.; Malick, D. K.; Rabuck, A. D.; Raghavachari, K.; Foresman, J. B.; Cioslowski, J.; Ortiz, J. V.; Stefanov, B. B.; Liu, G.; Liashenko, A.; Piskorz, P.; Komaromi, I.; Gomperts, R.; Martin, R. L.; Fox, D. J.; Keith, T.; Al-Laham, M. A.; Peng, C. Y.; Nanayakkara, A.; Gonzalez, C.; Challacombe, M.; Gill, P. M. W.; Johnson, B.; Chen, W.; Wong, M. W.; Andres, J. L.; Gonzalez, C.; Head-Gordon, M.; Replogle, E. S.; Pople, J. A. *Gaussian 98*, revision A.9; Gaussian, Inc., Pittsburgh, PA, 1998.
(25) Adamo, C.; Barone, V. *Chem. Phys. Lett.* **1997**, *274*, 242.
(26) Adamo, C.; Barone, V. *J. Chem. Phys.* **1998**, *108*, 664.
(27) Porembski, M.; Weisshaar, J. C. *J. Phys. Chem. A* **2001**, *105*, 6655.
(28) Porembski, M.; Weisshaar, J. C. *J. Phys. Chem. A* **2001**, *105*, 4851.
(29) Zhang, Y.; Guo, Z.; You, X.-Z. *J. Am. Chem. Soc.* **2001**, *123*, 9378.
(30) Dunbar, R. C. *J. Phys. Chem. A* **2002**, *106*, 7328.
(31) McLean, A. D.; Chandler, G. S. *J. Chem. Phys.* **1980**, *72*, 5639.
(32) Blaudeau, J.-P.; McGrath, M. P.; Curtiss, L. A.; Radom, L. *J. Chem. Phys.* **1997**, *107*, 5016.
(33) Hay, P. J. *J. Chem. Phys.* **1977**, *66*, 4377.
(34) Wachters, A. J. H. *J. Chem. Phys.* **1970**, *52*, 1033.
(35) Rhagavachari, K.; Trucks, G. W. *J. Chem. Phys.* **1989**, *91*, 1062.
(36) Feller, D. *Chem. Phys. Lett.* **2000**, *322*, 543.
(37) Xantheas, S. S. *J. Chem. Phys.* **1996**, *104*, 8821.
(38) Counterpoise corrections were calculated as follows (kcal mol^{-1}). Corannulene: Na η^5_{out}, 1.0; Na η^5_{in}, 1.8; Na η^6_{out}, 1.2; Ti η^5_{in}, 2.7; Ti η^6_{out}, 1.4; Ti η^6_{in}, 2.0; Cr η^6_{out}, 1.0; Cr η^6_{in}, 1.7; Ni η^5_{in}, 2.0; Ni η^6_{out}, 1.9; Ni η^6_{in}, 1.5; Cu η^2_{out}, 1.1. Coronene: Na, 1.1; K, 1.9; Cr, 1.7.
(39) There is possible ambiguity in referring to electrostatic interactions, because some literature considers the term "electrostatic interaction" to include the polarization interaction. Here, the polarization contribution is considered separately.
(40) Bauschlicher, C. W., Jr.; Partridge, H.; Langhoff, S. R. *J. Phys. Chem.* **1992**, *96*, 3273.
(41) Stone, A. J. *The Theory of Intermolecular Forces*; Clarendon Press: Oxford, 1996.
(42) Klarner, F.-G.; Panitzky, J.; Preda, D.; Scott, L. T. *J. Mol. Model.* **2000**, *6*, 318.